Finite Volume Method Study on Contact Line Jump Phenomena and Dynamic Contact Angle of Underfill Flow in Flip-Chip of Various Bump Pitches

Finite Volume Method Study on Contact Line Jump Phenomena and Dynamic Contact Angle of Underfill Flow in Flip-Chip of Various Bump Pitches

F C Ng[1], A Abas[1*] and M Z Abdullah[2]

[1] School of Mechanical Engineering, Universiti Sains Malaysia, Engineering Campus, 14300, Nibong Tebal, Penang, Malaysia.

[2] School of Aerospace Engineering, Universiti Sains Malaysia, Engineering Campus, 14300, Nibong Tebal, Penang, Malaysia.

Corresponding author *: aizatabas@usm.my

Abstract. Three distinct flip-chip underfill cases were considered in this work, with each possess a bump pitch of 0.8 mm, 1.0 mm and 1.2 mm. Contact line jump (CLJ) phenomenon during the underfill flow were successfully visualized with the aided of finite volume method (FVM) based simulation. The current simulated underfill flow fronts were qualitatively validated with the existing experimental data. Generally, the attachment process occurs much faster than the detachment process, by a factor of 14. Within the investigated pitches range, shorter bump pitch would yield a slower underfill flow but a faster-completion underfill process. The voiding mechanism during the underfill process were presented. Furthermore, the dynamic contact angle of underfill meniscus were analytically computed from the numerical data. The contact angle is found to be varies sinusoidally with the filling time, while the impact of bump pitch is minimal. Lastly, it is found that the bump pitch of flip-chip does affect the void formation and propagation.

***Keywords*:** Bump pitch; contact line jump (CLJ); dynamic contact angle; flip-chip encapsulation; underfill process

1. Introduction

To enhance the reliability electronic package and device, underfill encapsulation is performed during the assembly manufacturing process at the chip or substrate levels. During the underfill process, a special type of adhesive fluid is introduced to the gap beneath the chip and substrate, which prior hardening it would form a harden layer. This protective layer would solve the thermal mismatch issue and serves as mechanical resistance to the fragile joints of the chip device. Upon realizing the particular importance of this underfill process, several researches were conducted from various point-views and methodology, with an ultimate aim to optimize and enhance the process and subsequently the package reliability [1 – 7].

Contact line jump (CLJ) is a phenomenon occurred during the underfill meniscus approaching the bump array or detaching the bump. This was firstly discovered by Young [8-9] and later experimentally observed by Lee et al. [10-11]. Later, Yao et al. had incorporate the idea of CLJ in formulating new filling time model [12].

There are several literatures that studied the effect on solder bump pitch on the underfill flow. They concluded that the decrease in bump pitch of flip-chip will substantially increases the filling time [10-12]. Eventually, Wan et al. had analytically developed the concept of critical clearance of flip-chip for effective underfill process [13]. On other hand, the effect of contact angle on underfill flow is vital [14-15].

This paper is devoted to study the underfill encapsulation process in flip-chip of varying bump pitch using the finite volume method (FVM) numerical scheme. The current numerical model is quantitatively validated to the existing experimental data [10] on the entrance and exit flow fronts. Through simulation, the occurrence of CLJ and the influence of bump pitches can be investigated. Additionally, the contact angle of underfill flow front is determined. These findings may benefit the optimization and enhancement works on underfill process.

2. Numerical simulation

In this paper, the finite volume method (FVM) based commercial software, Ansys is adopted to numerically model the underfill flow during the flip-chip encapsulation process. Navier-Stokes (N-S) and continuity equations were governed and solved using the FVM scheme. On the side of mathematical model of flip-chip, there were three variations with different bump pitches, w of 0.8 mm, 1.0 mm and 1.2 mm (respectively dimensionless pitch, α of 1.6, 2.0 and 2.4). However, all flip-chips have same bump diameter, d of 0.5 mm and gap height, h of 0.45 mm. These flip-chip parameters were defined in Figure 1. Further, the solder bumps were in quadrilateral arrangement and a side length of 0.5 mm. The whole bump array is set at 3 × 2 so the flow meniscus can be securitized. The underfill flow pattern is repetitive along each row of bump, therefore only two rows were considered in current simulation. A Newtonian fluid of density 1600 kg/m^3, viscosity 1.5 Pa-s and surface tension, 0.012 N/m was used as the underfill material. The underfill fluid is continuously dispensed to the flip-chip along one edge side, mimicking the I-type single inlet dispensing method. The computational models were meshed with fine tetrahedral setting with proximity on. Multiphase volume of fluid (VOF) is chosen to track the advancement of flow front of underfill fluid. This underfill simulation is modelled to be transient, laminar and incompressible flow. The transient time step used is 0.01 s with a maximum of 20 iterations per time step. For boundary conditions set are: 0 Pa gauge pressure on both flow inlet and outlet, no-slip on walls and capillary pressure flow front. Lastly, the numerical simulated flow fronts will be compared with the existing experiment data by Lee et al. [10] on the flip-chip case with dimensionless pitch of 2.0. As validation, a qualitative comparison on the flow fronts at different filling stages (i.e. the attachment jump and detachment jump) was performed and presented in Figure 2.

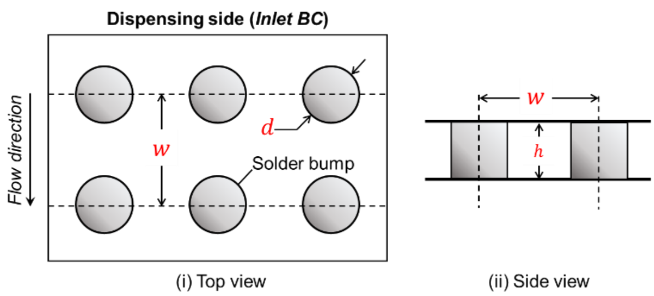

Figure 1. The geometrical representation of a flip-chip.

3. Result and Discussions

Figure 2 depicts the side-by-side comparison of experimental [10] and numerically simulated flow front of underfill fluid in the flip-chip with linear density, $\alpha = 2$.This serves as a validation study to qualitatively verify the accuracy of numerical model and subsequent findings. It is found that the simulated flow fronts are in great consensus with the experimental findings at respective filling stages in terms of meniscus shape and flow front position. Our numerical simulation also able to capture the occurrence of contact line jump in both the entrant and exit (as in Figure 2 (**ii**) and Figure 2 (**iv**) respectively), similarly to that being reported in the experimental works [10].

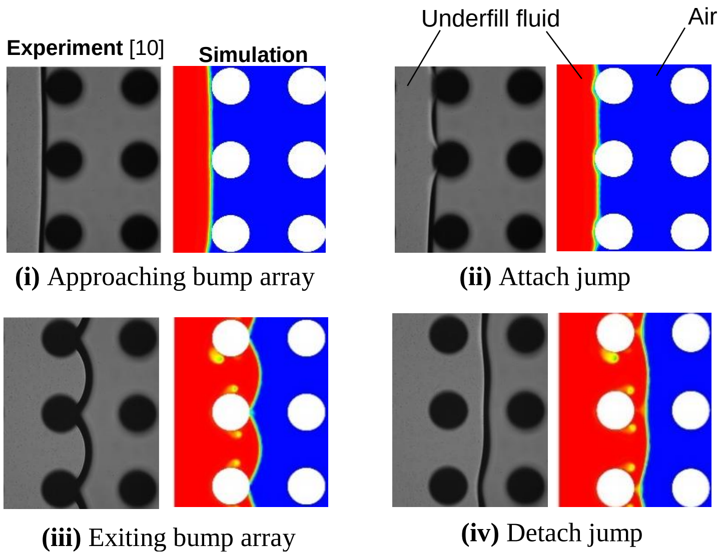

Figure 2. Validation study of simulated flow front (right) of underfill front in flip-chip bump array by comparing to the corresponding experimental flow fronts (left) by Lee et al. [10], for different filling stages of underfill flow.

Figure 3 gives the filling time plots for the underfill flow at various filling stages, for instance attachment, propagation & voiding and detachment. Generally, all filling time plots show monotonically increasing trend. On the trending of bump pitches, smallest bump pitches constitute for the longest filling time as evident in the flip-chip case of 0.8 mm pitch, which is consistent with the conclusions attained by past literatures [10 – 12]. The narrow gap between two adjacent bumps in flip-chip of lower pitch is found to be substantially hindering the detachment process; while the effect of bump pitch on bump attachment process is not significant. Besides, it is found that the attachment jump when the flow front first approach the bump array occurred instantaneously, within 0.05 s (refers Table 1). On contrary, the detachment jump is a slow process, where the flow front took up to 0.70 s to detach away from the bump array (see Table 3). Furthermore, the overall trend of underfill fluid flow across the bump array is decelerating, as being exhibited by the exponential curve in filling time plot in Figure 3.

During the propagation of underfill fluid across the bump array, voids start to form due to the interaction with bump surface by the entrapment of air. Table 2 depicts the voids formed after the underfill flow entered bump array. It is found that the air voids tend to form behind the solder bump, as the flowing underfill fluid is being obstructed by the bump array. Such inelastic collision with the solder bump not only reduces the flow rate, but also cause the formation of undesired defect – air void – which is potent to the package reliability.

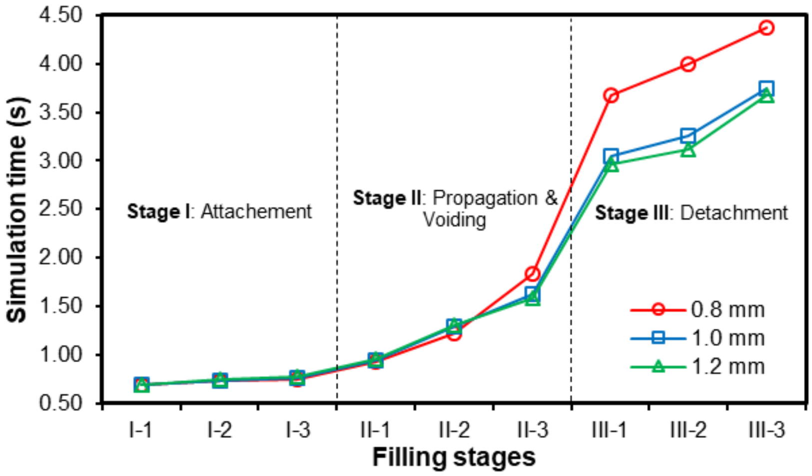

Figure 3. Filling time plots of underfill flow at three filling stages for flip-chips with bump pitches of 0.8 mm, 1.0 mm and 1.2 mm.

Table 1. Stage I – underfill meniscus attachment to the solder bump.

	$w = 0.8$ mm $\alpha = 1.6$	$w = 1.0$ mm $\alpha = 2.0$	$w = 1.2$ mm $\alpha = 2.4$
Stage I-1: Entrance ($x' = 0$)	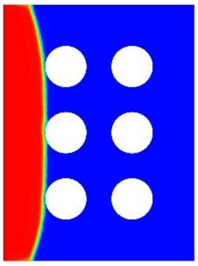 0.69 s	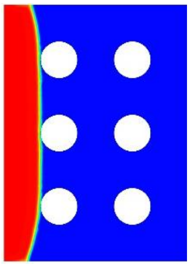 0.69 s	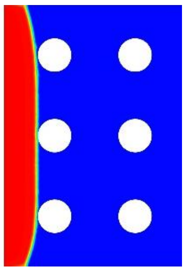 0.69 s
Stage I-2: Jump (Attach)	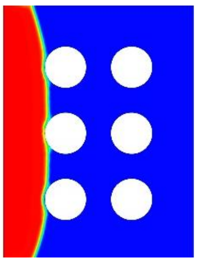 0.73 s	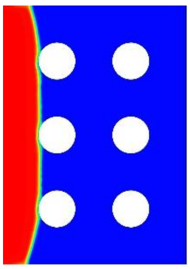 0.73 s	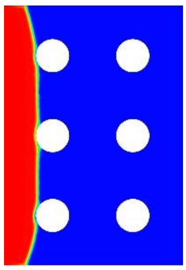 0.74 s
Stage I-3: Meniscus curved	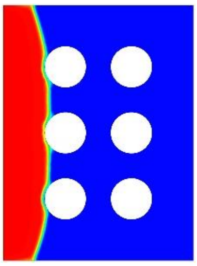 0.75 s	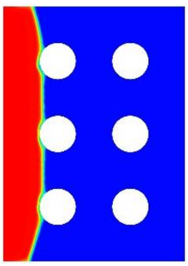 0.76 s	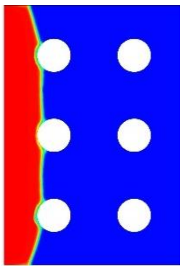 0.77 s

IOP Conf. Series: Materials Science and Engineering **530** (2019) 012012 doi:10.1088/1757-899X/530/1/012012

Table 2. Stage II – propagation of underfill meniscus and void formation.

	$w = 0.8$ mm $\alpha = 1.6$	$w = 1.0$ mm $\alpha = 2.0$	$w = 1.2$ mm $\alpha = 2.4$
Stage II-1: Mid-bump $\left(x' \approx \frac{d}{2}\right)$	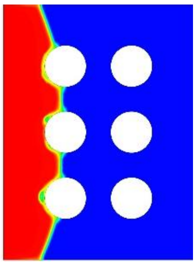 0.93 s	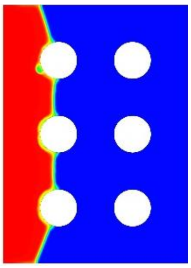 0.94 s	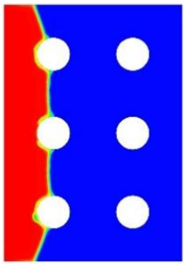 0.96 s
Stage II-2: Voiding	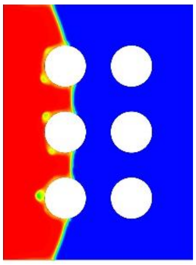 1.22 s	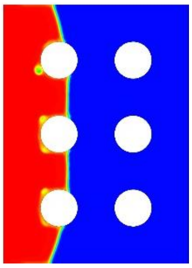 1.29 s	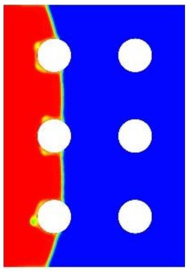 1.31 s
Stage II-3: Exit $(x' \approx d)$	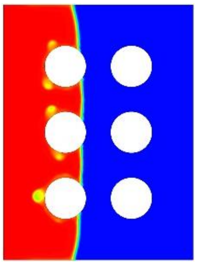 1.84 s	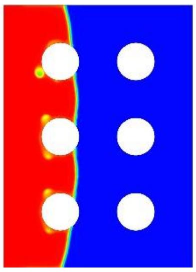 1.62 s	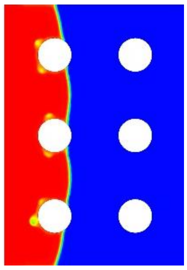 1.58 s

Figure 4 presents the plot of volume fraction filled by the underfill fluid at different filling time for all three flip-chips system. The simulation data were fitted into polynomial equations with a high correlation coefficient of $R > 0.998$. It is observed that in the flip-chip of lowest bump pitch (i.e. 0.8 mm) yields highest volume fraction filled by underfill fluid over the time. This appeared to be contradicted to the finding in Figure 3. Such discrepancy is caused by the fact the total volume of flip-chip with smaller bump pitch is lower. Therefore, upon comparing the volume fraction filled, an opposite trend is being observed instead. It is interesting to observed that the total volume of flip-chip outweighed the influence of bump pitch on the filling time. Therefore, the underfill process of flip-chip with smaller bump pitch can be completed faster, but not account for faster underfill flow.

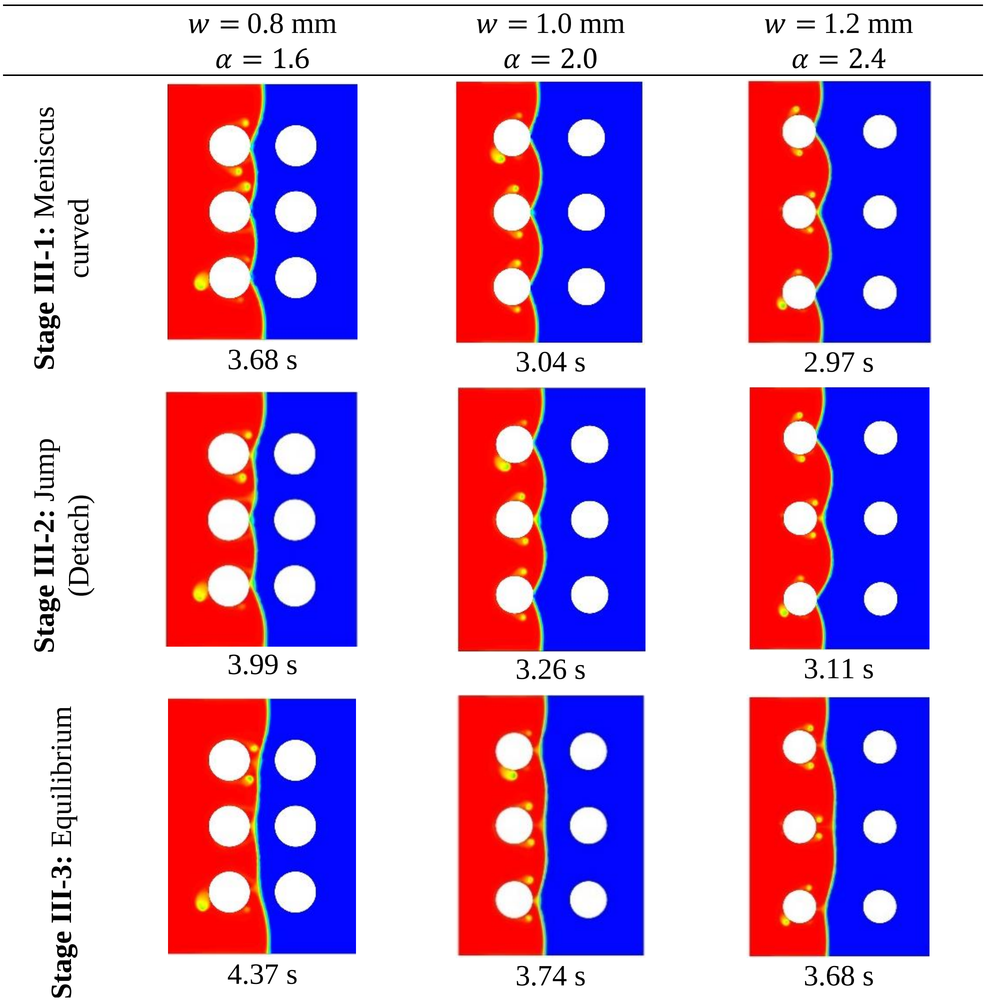

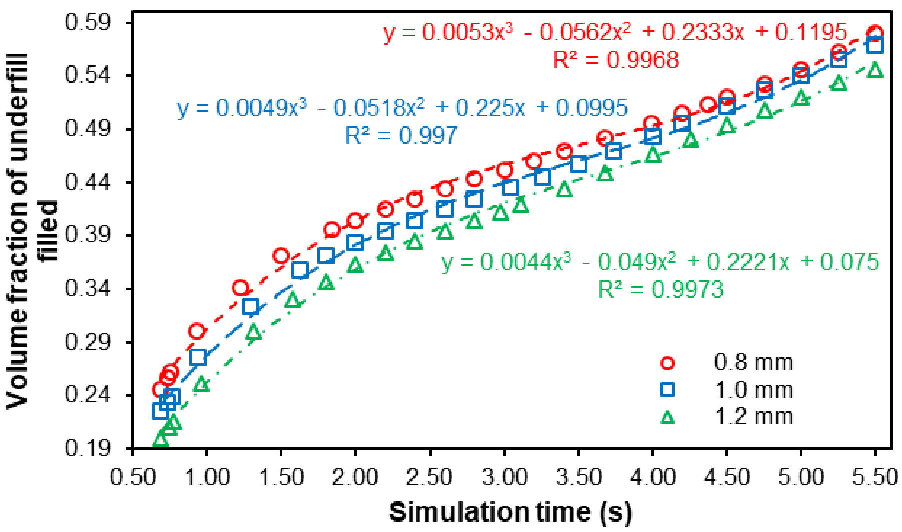

Figure 4. Plot of underfill-filled volume fraction against time for the flip-chip of different bump pitches: 0.8 mm, 1.0 mm and 1.2 mm.

Figure 5 shows the side-view of the underfill flow in the gap between substrate and flip-chip, together with its geometrical representation to analytically compute the contact angle, θ. By trigonometry, the angle can be mathematically written as follows:

$$\theta = \cos^{-1}\left[\frac{4\beta}{1+4\beta^2}\right], \quad (1)$$

where $\beta = t/h$. The contact angle of the underfill meniscus at different time for all three flip-chips were computed and plotted in Figure 6. A sinusoidal trend is observed for the plot of contact angle against time. This inferred the contact angle of the underfill fluid is not statics but rather dynamic, strongly influenced by the flow time. However, there is no significant effect of bump pitches on the variation of contact angle. The dynamic contact angle is an intrinsic material property of the underfill fluid itself, and not bounded to the geometrical parameter of the flip-chip.

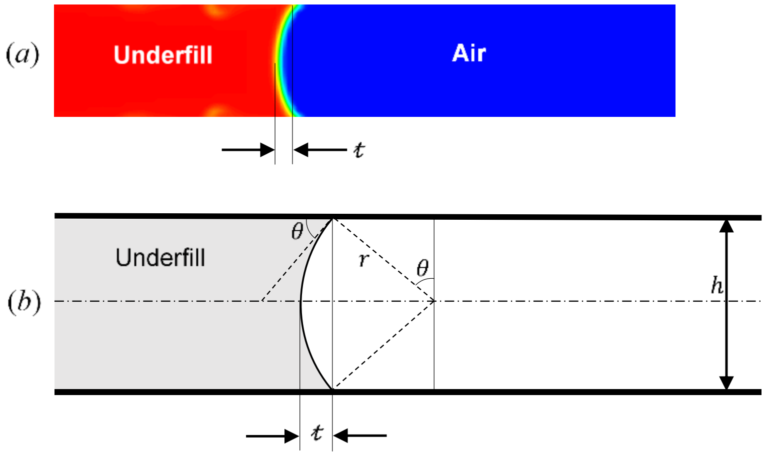

Figure 5. Measurements of meniscus's contact angle, θ from (*a*) the simulated VOF flow front; (*b*) the geometrical interpretation of underfill's meniscus, as viewed from the side.

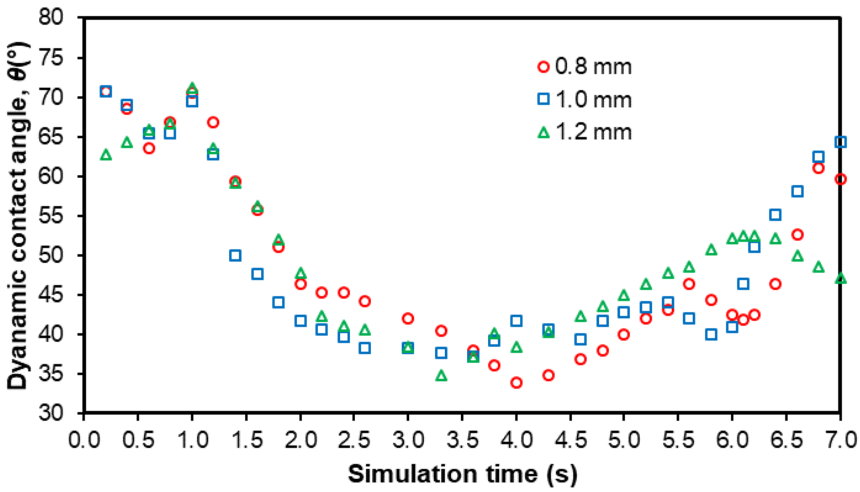

Figure 6. Plot of dynamic contact angle of underfill fluid meniscus at different filling time, for flip-chips with various bump pitches.

Figure 7 depicts the VOF and gauge pressure contours for three flip-chip cases at the time of 5.00 s. Consistent to the boundary conditions applied, the flow front's gauge pressure is negative due to the capillary action while the unfilled air region is at the atmospheric pressure of 0 Pa. The air void is found to possess a positive gauge pressure. Void is a sack of compressed air that being surrounded by the underfill fluid. The dynamic propagation of the air void formed in each flip-chip cases were quantitatively visualized in Figure 8. It is found that the initial position of the void formed significantly affects its propagation, such that the void that formed directly behind the bump ($\varphi < 90°$) would travels slower to escape the vicinity of bump ($\varphi > 180°$). The initial void favours to form at directly behind the bump for the flip-chip configuration with the shortest bump pitch of 0.8 mm (Void 1).

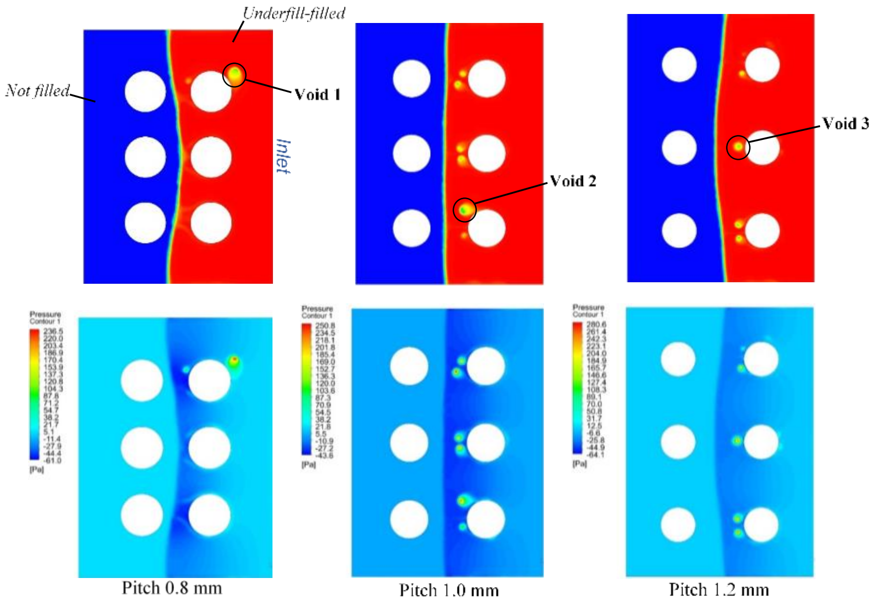

Figure 7. Underfill volume fraction profiles and pressure distributions at the stage IV at the simulation time of 5.00 s. Three air voids, with each from array of different bump pitch, were circled and marked as Void 1, Void 2 and Void 3 respectively.

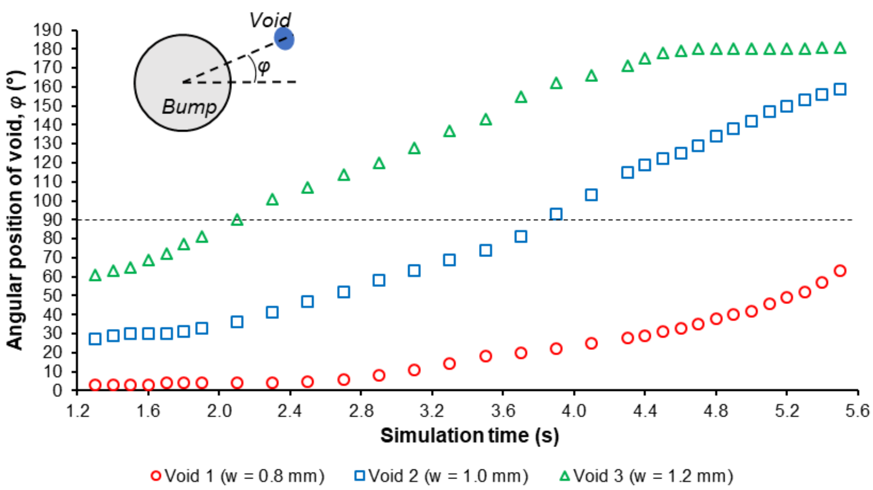

Figure 8. The plot of angular positions of Void 1, Void 2 and Void 3 (respectively from bump array with pitches $w = 0.8$ mm, $w = 1.0$ mm and $w = 1.2$ mm) relative to the center of solder bump.

4. Conclusions

Using finite volume method (FVM) based numerical scheme, the underfill flow across the bump array are successfully simulated alongside with the contact line jump (CLJ) phenomenon during both the attachment and detachment. In term of filling time, detachment process is significantly much slower than the attachment process. The effect of bump pitch on the filling time of underfill flow is investigated by consider the flip-chips of different pitches: 0.8 mm, 1.0 mm and 1.2 mm. It is revealed that lower pitch leads to slower underfill flow but faster completion of the underfill process. The bump pitch is found to affect the detachment process to a significant extend, where the time taken for the meniscus to detach away from the bump is higher in flip-chip with small pitch. Besides, the voiding process during the advancement of underfill along the bump array is observed from the current simulation work. Undesired defect – void – is formed due to the entrapment of air during the underfill fluid first contact with the solder bump. Lastly, the variation of contact angle of underfill fluid along the filling time is analysed and found that the contact angle varies in a sinusoidal manner. These findings justified that the FVM numerical simulation is capable in study the underfill flow from the viewpoints of CLJ, void and dynamic contact angle.

Acknowledgement:

This work was partly supported by the FRGS grant FRGS/1/2015/TK03/USM/03/2 and USM Research University Grant 8014071 from the Division of Research and Innovation, University Sains Malaysia, Engineering Campus, Penang. Additionally, the authors would like to acknowledge the financial support from the USM Fellowship 2017/18 scheme, provided by the Institute of Postgraduate Studies (IPS), Universiti Sains Malaysia (USM).

References:

[1] F C Ng, A Abas, M H H Ishak, M Z Abdullah and M S Abdul Aziz 2016 Effect of Thermocapillary Action in the Underfill Encapsulation of Multi-stack Ball Grid Array *Microelectronics Reliability* Vol 66 pp 143 – 160

[2] F C Ng, A Abas, Z L Gan, M Z Abdullah, F Che Ani and M Yusuf Tura Ali 2017 Discrete phase method study of ball grid array underfill process using nano-silica filler-reinforced composite-encapsulant with varying filler loadings *Microelectronics Reliability* Vol 72C pp 45 – 64

[3] F C Ng, M A Abas, M Z Abdullah, M H H Ishak and G Y Chong 2017 CUF scaling effect on contact angle and threshold pressure *Soldering & Surface Mount Technology* Vol 29 Issue 4 pp 173 – 190

[4] F C Ng, A Abas and M Z Abdullah 2018 Effect of solder bump shapes on underfill flow in flip-chip encapsulation using analytical, numerical and PIV experimental approaches *Microelectronics Reliability* Vol 81 pp 41 – 63

[5] A Abas, F C Ng, Z L Gan, M H H Ishak and G Y Chong 2018 Effect of scale size, orientation type and dispensing method on void formation in the CUF encapsulation of BGA *Sadhana* Vol 43 Issue 4 No 59

[6] J W Wan, W J Zhang and D J Bergstrom 2009 Numerical Modeling for the Underfill Flow in Flip-Chip Packaging *IEEE Transactions on Components and Packaging Technologies* Vol 32 No 2 pp 227 – 234

[7] CY Khor, M Z Abdullah, M Abdul Mujeebu and F Che Ani 2010 FVM based numerical study on the effect of solder bump arrangement on capillary driven flip chip underfill process *International Communications of Heat and Mass Transfer* 37 pp 281 – 286

[8] W B Young 2003 Anisotropic behavior of the capillary action in flip chip underfill *Microelectronics Journal* Vol 34 no 11 pp 1031 – 1036

[9] W B Young 2004 Capillary impregnation into cylinder banks *Journal of Colloid and Interface Science* Vol 273 pp 576 – 580

[10] S H Lee, J Sung and S E Kim 2010 Dynamic flow measurements of capillary underfill through a bump array in flip chip package *Microelectronics Reliability* Vol 50 No 12 pp 2078 – 2083

[11] Y B Kim, J Sung and M H Lee 2011 Micro-PIV measurements of capillary underfill flows and effect of bump pitch on filling process *Journal of Visualization* Vol 14 No 3 pp 237 – 248

[12] X J Yao, Z D Wang and W J Zhang 2014 A new analysis of the capillary driving pressure for underfill flow in flip-chip packaging *IEEE Transactions on Components, Packaging and Manufacturing Technology* Vol 4 No 9 pp 1534 – 1544

[13] J W Wan, W J Zhang and D J Bergstrom 2007 A theoretical analysis of the concept of critical clearance toward a design methodology for the flip-chip package *Journal of Electronic Packaging* Vol 129 pp 473 – 478

[14] W B Young and W L Yang 2006 Underfill of flip-chip: the effect of contact angle and solder bump arrangement *IEEE Transactions on Advanced Packaging* Vol 29 No 3 pp 647 – 653

[15] J Wang 2002 Underfill of flip chip on organic substrate: viscosity, surface tension, and contact angle *Microelectronic Reliability* Vol 42 pp 293 – 299